

# Analytical Methods

Accepted Manuscript



This is an *Accepted Manuscript*, which has been through the Royal Society of Chemistry peer review process and has been accepted for publication.

*Accepted Manuscripts* are published online shortly after acceptance, before technical editing, formatting and proof reading. Using this free service, authors can make their results available to the community, in citable form, before we publish the edited article. We will replace this *Accepted Manuscript* with the edited and formatted *Advance Article* as soon as it is available.

You can find more information about *Accepted Manuscripts* in the [Information for Authors](#).

Please note that technical editing may introduce minor changes to the text and/or graphics, which may alter content. The journal's standard [Terms & Conditions](#) and the [Ethical guidelines](#) still apply. In no event shall the Royal Society of Chemistry be held responsible for any errors or omissions in this *Accepted Manuscript* or any consequences arising from the use of any information it contains.

## Hyphenated techniques of thermal analysis for dibenz [b, f] [1, 4] oxazepine

Tian Xue <sup>a,b</sup>, Qing-zhong Cui<sup>a</sup>, Yong-he Han<sup>b</sup>, Shan Wang<sup>b</sup>, Yong-yang Mao<sup>b</sup>

(a. State Key Laboratory of Explosion Science and Technology, Beijing Institute of Technology, Beijing, China;

b. 61699 Unit, PLA, Zhijing, China)

**Abstract:** As a third-generation tear agent, dibenz [b, f] [1, 4] oxazepine (CR) has been widely used for anti-terrorism and riot control efforts. To improve the efficiency of CR use and determine the toxicity of its decomposition products, it is necessary to study its thermal stability and thermal decomposition behaviour. The mass loss and thermal behaviour of CR were studied at different heating rates using, the thermogravimetry (TGA) and the differential scanning calorimetry (DSC) techniques. The gas products were analyzed using Fourier transform infrared spectroscopy (FTIR). The present work also studied the thermal decomposition characteristics of CR for temperatures in the 200-600 °C range using the pyrolysis-gas chromatography/mass spectrometry (PY-GC/MS) technique, and the decomposition products were identified. The results show that, CR fuses at approximately 69 °C, and that the heating rate has a relatively strong influence on the extrapolated initial decomposition temperature. In the absence of oxygen, when the heating rate is 2 °C·min<sup>-1</sup>, CR starts to decompose at 172 °C. The mechanism of the thermal decomposition is described by the Zhuralev-Lesokin-Tempelmann equation,  $f(\alpha) = \frac{3}{2}(1-\alpha)^{\frac{2}{3}} \left[ (1-\alpha)^{\frac{1}{3}} - 1 \right]^{-1}$ , and the activation energy is approximately 230 kJ·mol<sup>-1</sup>. In the thermal pyrolysis experiment, the first step of thermal decomposition of CR occurs between 200 and 300 °C. Below 600 °C, in an aerobic environment, the pyrolysis reaction occurs to produce 2-aminodiphenyl ether, whereas the oxidizing reaction occurs to produce 10, 11-dihydrodibenz [b, f] [1, 4] oxazepin-11-one, with the products obtained independent of temperature. According to the experimental results, the burning temperature for the mixture of CR and the fireworks is suggested to be below 200 °C.

**Keywords:** dibenz [b, f] [1, 4] oxazepine; thermal decomposition; thermogravimetry(TGA); differential scanning calorimetry(DSC); Fourier transform infrared spectroscopy(FTIR); pyrolysis-gas chromatography/mass spectrometry(PY-GC/MS)

### Introduction

Dibenz [b, f] [1, 4] oxazepine was synthesized for the first time by Higginbotton and Suschitzky in 1962<sup>1</sup>, and its American code is CR (the chemical structure is show in Fig. 1). Similar to irritants such as CN (Chloroacetophenone) and CS (2-Chlorobenzalmalononitrile), the third-generation riot control agent CR can produce irritation to the eyes, nose, skin and throat at low concentrations. However, compared with the other two irritants, CR is less toxic and has a larger safe range<sup>2-4</sup>. CR was used to equip American police in 1974. In recent years, non-lethal weapons filled with irritant have played an important role in the increasingly demanding anti-terrorism and riot control efforts<sup>5,6</sup>.

1  
2  
3 In practical applications, the ammunition charge is composed of CR and incendiary agents or explosives. CR  
4 is spread in the air by heating or explosions to produce aerosols that can effectively disperse a riot<sup>7</sup>. Both the  
5 burning of incendiary agents and the explosion process of explosives can produce high temperatures. The burning  
6 temperatures of incendiary agents range from hundreds to thousands of degrees centigrade<sup>8,9</sup>, and the explosives'  
7 explosion temperatures also can reach thousands of degrees, though they have a short duration<sup>10</sup>. Thus, in these  
8 applications, CR is decomposed while it is dispersed by the effects of burning or explosion. Additionally, CR is  
9 also used in rodent resistance coatings for power cables. In order to prolonging service life of cables under high  
10 temperatures caused by thermoelectric effects, it is of great importance to evaluate the thermal stability of CR.  
11 Therefore, it is of practical significance to study the thermal decomposition of CR and identify its decomposition  
12 products at different temperatures. In this study, the theoretical basis for the formulae is first provided. CR  
13 decomposition can be reduced by adjusting the temperatures of burning or exploding, thus improving the soft  
14 lethal power of the ammunition. Second, for better CR use, it is helpful to identify the decomposed products and  
15 determine their toxicity to the human body. Third, the proper temperature can be selected when using the  
16 incineration method to destroy waste tear bombs to reduce environmental pollution by controlling the incineration  
17 bottom ashes<sup>11,12</sup>.

18  
19  
20  
21  
22  
23  
24  
25  
26  
27  
28  
29  
30  
31  
32  
33  
34  
35  
36  
37  
38  
39  
40  
41  
42  
43  
44  
45  
46  
47  
48  
49  
50  
51  
52  
53  
54  
55  
56  
57  
58  
59  
60  
There are many reports in the literature on the synthesis of stimulants such as CR<sup>13,14</sup> and its stimulant  
function toward an organism<sup>15,16</sup>. Makles studied the examination and recognition of CR<sup>17</sup>, and Zuo investigated  
the oxidation products of CR<sup>18</sup>. However, there have been fewer studies on the stability and thermal  
decomposition of the stimulants. Kluchinsky et al. collected the pyrolysate of CS using the PTFE filter and  
analyzed the composition of the pyrolysate using gas chromatography–mass spectrometry (GC/MS); however,  
they did not explain the specific temperature observed during the thermal decomposition<sup>19</sup>. They then studied the  
possible generation of HCN and HCl during the thermal decomposition of CS at high temperatures (over  
700 °C)<sup>20</sup> and the products of the thermal decomposition of CS at the temperatures in the 300-900 °C range using  
the tubular furnace and GC/MS techniques<sup>21</sup>. Hook et al. studied the relation between the decomposition products  
and temperatures by collecting and analyzing the products of the thermal decomposition of CS in the 150-300 °C  
range using solid phase microextraction and GC/MS<sup>22</sup>. A systematic analysis of CR decomposition at a specified  
temperature is scarcely found in the publicly available literature. Moreover, the current methods for analyzing the  
thermal decomposition of stimulants such as CS do not apply to CR. The thermal decomposition of CR exhibits  
unique characteristics: the second reaction occurs if the heating rate is not sufficiently high to deliver the  
thermolysis products into the chromatograph before the specified temperature, for example, 500 °C. In this case, it

is difficult to determine the real thermal decomposition mechanism of CR at this temperature. Therefore, a new analysis method must be used.

In the present work, the thermolysis function of CR was first comprehensively investigated. The weight loss and corresponding heat effect were studied by simultaneous TGA/DSC at low CR heating, and its emergent gas was analyzed by FTIR. The PY-GC/MS technique can be used to study CR thermal decomposition at a certain temperature and identify its decomposition product. In the experiment, the thermal pyrolysis unit heated rapidly at the rate of  $3000\text{ }^{\circ}\text{C}\cdot\text{s}^{-1}$ , upon reaching the set temperature, the sample free-fell into the pyrolysis bottle. The weight of the sample used in the experiment was measured with  $\mu\text{g}$  precision, and the dead volume of the pyrolysis unit was small, with a low density of its pyrolytic products. The above aspects ensured the thermal decomposition of CR at a precise temperature, decreased the secondary reaction of products to the greatest possible extent, and could better simulate the thermal decomposition of the irritants during the burning of pyrotechnic compositions and explosive detonation<sup>23</sup>.

## Experiments

### Main Instruments and Devices

449F3 Type TG/DSC Simultaneous Thermal Analyzer: German Netzsch Corporation, temperature range:  $-120\sim 2400\text{ }^{\circ}\text{C}$ ; mass resolution:  $0.1\text{ }\mu\text{g}$ , heat flow sensitivity:  $<1\text{ }\mu\text{W}$ , heating rate:  $0.001\sim 50\text{ }^{\circ}\text{C}\cdot\text{min}^{-1}$ , vacuum degree:  $10\sim 4\text{ mbar}$ ; temperature of connector with infrared: room temperature $\sim 300\text{ }^{\circ}\text{C}$ . VERTEX70V infrared spectrometer: German Bruker Corporation, beam splitter: KBr-on-Ge, detector: MCT type, spectral range:  $25,000\sim 20\text{ cm}^{-1}$ , spectral resolution:  $0.4\text{ cm}^{-1}$ , rapid scanning rate:  $80\text{ file}\cdot\text{s}^{-1}$  ( $16\text{ cm}^{-1}$  resolution), wavenumber accuracy:  $0.01\text{ cm}^{-1}$ , temperature of gas cell in situ and joint transfer line:  $230\text{ }^{\circ}\text{C}$ ; room temperature. GCMS-QP2010SE Gas Chromatography Mass Spectrometer: Produced by Shimadzu Corporation in Japan; EGA/PY-3030D Pipe Furnace Pyrolyzer: Produced by Frontier in Japan.

### Main Materials

Dibenz [b, f] [1, 4] oxazepine (its molecular formula is  $\text{C}_{13}\text{H}_9\text{NO}$ , its CAS number is 257-07-8, its purity is 97% with a pure chromatographic, and it is yellow powder): Produced by Nan Xing Chemical Plant in Hubei.

### Experimental Conditions

#### TGA/DSC-FTIR

An aluminum pool was used as the crucible of the thermoanalyzer, and argon was used as the purging gas. Purge

1  
2  
3 gas flow: 50 mL·min<sup>-1</sup>; protect gas flow: 25 mL·min<sup>-1</sup>. Temperature range: 50~350 °C, heating rate: 2, 5,  
4 10 °C·min<sup>-1</sup>, sample quality: 5 mg. The selected wave number range in FTIR is 4000~650 cm<sup>-1</sup>, and the  
5  
6 temperature of the infrared gas pool and combined transmission line is 200 °C.  
7

### 8 9 **PY-GC/MS**

10  
11 Pyrolytic condition: the pyrolysis temperature range is 200~600 °C, with 100 °C as the step size; the pyrolysis  
12 time is 30 s. The pyrolyzer is filled with air inside, and the carrier gas is argon. Chromatographic condition: Ultra  
13 alloy-5 type capillary column (30 m×0.25 mm×0.25 μm) produced by Agilent Corporation; the temperature  
14 programming uses the temperature of the injection port, and the starting temperature of the sample is 50 °C. The  
15 temperature is maintained for 1min and is then raised to 300 °C at a rate of 8 °C·min<sup>-1</sup>, where it is maintained for  
16 4 min; the flow rate of the purging gas (argon) is 2 mL·min<sup>-1</sup>. Mass spectra condition: ion source: EI, electron  
17 energy 70 eV; scanned area: m/z 33~600; detector temperature 250 °C.  
18  
19  
20  
21  
22  
23

### 24 25 **Results and Discussions**

#### 26 27 **TGA/DSC**

28  
29 **Fig. 2** shows the TGA and DSC curves of CR when the temperature is raised from 50 °C to 350 °C at different  
30 heating rates ( $\beta=2, 5, 10$  °C·min<sup>-1</sup>).  
31  
32

#### 33 34 **Analysis of Heating Process**

35 An examination of **Fig. 2** shows that the TGA curve exhibits only one step between 170 and 230 °C and that the  
36 mass loss of sample is approximately 80%. In this stage, a continuous thermal CR decomposition reaction occurs.  
37 As the heating rate  $\beta$  increases, the extrapolated initial weight loss temperature  $T_0$  on the TGA curve tends to  
38 move toward higher temperatures. The DSC curve shows one endothermic peak at 67-70 °C with no mass change,  
39 corresponding to a melting peak. As the heating rate is increased, no obvious rearward movement is observed for  
40 the melting peak. The endothermic peak appears between 170 and 230 °C. This temperature range corresponds to  
41 the weight loss step of the TGA curve. This peak shows the trend of rearward movement with the increasing  
42 heating rate. **Table 1** shows the melting peak values and the extrapolated initial weight loss temperatures for the  
43 different heating rates.  
44  
45  
46  
47  
48  
49  
50  
51

#### 52 53 **Kinetic Parameters of the Thermal Decomposition**

54 The formulas of Kissinger's method and Flynn-Wall-Ozawa's method are as follows:  
55

56 Kissinger's method<sup>24</sup>:  
57  
58  
59  
60

$$\ln \left[ \frac{\beta}{T_p^2} \right] = \ln \frac{A_K R}{E_K} - \frac{E_K}{R} \frac{1}{T_p}$$

where  $\beta$  is the heating rate ( $^{\circ}\text{C}\cdot\text{min}^{-1}$ ),  $T_p$  is the peak decomposition temperature (K),  $A_K$  is the pre-exponential factor ( $\text{s}^{-1}$ ),  $E_K$  is the activation energy ( $\text{kJ}\cdot\text{mol}^{-1}$ ), and  $R$  is the ideal gas constant ( $\text{J}\cdot\text{mol}^{-1}\cdot\text{K}^{-1}$ ).

Flynn-Wall-Ozawa's method<sup>25,26</sup>:

$$\lg \beta = \lg \left( \frac{AE_O}{RG(\alpha)} \right) - 2.315 - 0.4567 \frac{E_O}{RT}$$

where  $\beta$  is the heating rate ( $^{\circ}\text{C}\cdot\text{min}^{-1}$ ),  $\alpha$  is the degree of conversion,  $G(\alpha)$  is the integrated form of the kinetics mechanism function,  $E_O$  is the activation energy ( $\text{kJ}\cdot\text{mol}^{-1}$ ), and  $R$  is the ideal gas constant ( $\text{J}\cdot\text{mol}^{-1}\cdot\text{K}^{-1}$ ).

When the calculation is carried out using the Kissinger method, a straight line can be obtained in a plot of  $\ln[\beta/T_{pi}]$  versus  $1/T_{pi}$ .  $E_K$  is then obtained from the slope, and  $A_K$  is obtained from the intercept. When it was calculated using the Flynn-Wall-Ozawa equation, the peak temperatures  $T_p$  of the DTG data were found to be almost equal to the corresponding values obtained for different  $\beta$  such that the value of  $E_O$  could also be determined using the linear relationship of  $\ln\beta$  and  $1/T$ . The results obtained using the verified Kissinger and Flynn-Wall-Ozawa calculation methods for the different heating rates ( $\beta=2, 5, 10$   $^{\circ}\text{C}\cdot\text{min}^{-1}$ ) are presented in **Table 2** ( $r$  is the linear relation coefficient).

### Determination of the most probable operating mechanism

Take the 41 mechanism function  $G(\alpha)$ <sup>27</sup> into the 4 integral methods:

Ordinary Integra method<sup>28</sup>:

$$\ln \left[ \frac{G(\alpha)}{T^2} \right] = \ln \left[ \frac{AR}{\beta E} \left( 1 - \frac{2RT}{E} \right) \right] - \frac{E}{RT}$$

Šatava-Šesták's method<sup>29</sup>:

$$\lg G(\alpha) = \lg \frac{AE}{R\beta} - 2.315 - 0.4567 \frac{E}{RT}$$

Coats-Redfern's method<sup>30</sup>:

$$\ln \left[ \frac{G(\alpha)}{T^2} \right] = \ln \left( \frac{AR}{\beta E} \right) - \frac{E}{RT}$$

Agrawal's method<sup>31</sup>:

$$\ln \left[ \frac{G(\alpha)}{T^2} \right] = \ln \left\{ \frac{AR}{\beta E} \left[ \frac{1 - 2\left(\frac{RT}{E}\right)}{1 - 5\left(\frac{RT}{E}\right)^2} \right] \right\} - \frac{E}{RT}$$

Using the iterative and linear least squares methods, the activation energy  $E$ , pre-exponential factor  $A$  and correlation coefficient  $r$  can be obtained. The available  $E$ ,  $\ln A$  and correlation index values can be used to

determine the most probable mechanism<sup>32</sup>. To determine the most probable mechanism of the CR's heat dissolution among the 41 organic functions, the following must be obeyed: (1) the difference between the kinetic parameters of the 4 integral methods and those obtained by the Kissinger and Flynn-Wall-Ozaw methods is small; (2) the correlation coefficient is greater than 0.98; and (3) the obtained E and A values conform to the general law of heat dissolution<sup>27, 33</sup>.

According to the result of comparative analyses, the thermal decomposition process of CR is that of three-dimensional diffusion, and the most probable mechanism is described by the Zhuralev-Lesokin-Tempelman equation given by  $f(\alpha) = \frac{3}{2}(1-\alpha)^{\frac{4}{3}} \left[ (1-\alpha)^{\frac{1}{3}} - 1 \right]^{-1}$ , with its integrated form given by  $G(\alpha) = \left[ (1-\alpha)^{\frac{1}{3}} - 1 \right]^2$ . The kinetic parameters listed in **Table 3** are obtained using the equation for the most probable mechanism.

### FTIR spectrum

**Fig. 3** shows the three-dimensional infrared spectrogram of the overflowed gas when the CR temperature increases from 50 °C to 700 °C at a rate of 5 °C·min<sup>-1</sup>. It can be seen from the figure that the entire spectrogram is composed of three stages in the heating process. The first stage is the phase from 0 s to 1178 s, in which there is no obvious absorption peak in the spectra, corresponding to the process prior to the CR decomposition. The second phase is from 1178 s to 3880 s, where several absorption peaks appear in the spectra but the relative locations of the peaks do not show any changes, with only changes in absorption intensity. The intensity peak value is around 2308 s, and **Fig. 4** shows a two-dimensional spectrogram indicating the locations of peak values. This part corresponds to the thermal analysis process in the 170~230 °C temperature range and it can be seen that the relative position of the absorption peak does not change. This means that the composition of the evolved gases generated by the CR thermal decomposition has not changed. The third phase is from 3880 s to 7000 s, where the relative locations of the absorption peaks of the spectra show no apparent change relative to the second phase, but the absorption strength weakens obviously, corresponding to the residual overflowed gas.

The conclusions of the spectrum analysis are as follows: the peaks at  $\sigma=3502$  and  $3407$  cm<sup>-1</sup> correspond to the stretching vibration of  $-\text{NH}_2$ , where the absorption intensity is relatively weak; the peaks at  $\sigma=3077$  and  $3031$  cm<sup>-1</sup> correspond to the stretching vibration of the benzene ring  $=\text{CH}$ , where the absorption intensity is also relatively weak; and the peaks at  $\sigma=1623$ ,  $1475$  and  $1452$  cm<sup>-1</sup> correspond to the stretching vibration of the benzene ring  $=\text{CH}$ , where the absorption intensity is relatively strong. The peak at  $\sigma=1265$  cm<sup>-1</sup> corresponds to the in-plane bending vibration of the benzene ring, where medium absorbance is observed. The peaks at  $\sigma=1228$  and  $1203$  cm<sup>-1</sup> correspond to flexible vibration of  $\text{C}-\text{O}-\text{C}$ , where the absorbance is strongest. The peaks at  $\sigma=1105$

1  
2  
3 and  $1033\text{ cm}^{-1}$  correspond to the single bond flexible vibrations of C-N and C-C, for which the absorbance is  
4 relatively weak. More peaks are observed for  $\sigma < 966\text{ cm}^{-1}$ , most of which are attributed to bending vibrations both  
5 outside and on the surface of benzene ring= $\text{CH}$ . Among these, the peak at  $\sigma = 765\text{ cm}^{-1}$  shows the highest  
6 absorbance, most likely caused by a high number (4) of adjacent groups on the benzene ring. According to the  
7 above analysis, the spectra presented in **Figs. 3** and **4** are inferred to be the infrared spectra of 2-Aminodiphenyl  
8 ether.  
9

#### 10 11 12 13 14 **PY-GC/MS**

15  
16  
17 When the thermoanalysis technique is applied to study the thermal decomposition of substances, a regular pattern  
18 of thermal decomposition under the conditions of a low temperature and a slow heating rate can be obtained.  
19 However, the use of CR is usually mixed with incendiary agents and explosives, and its decomposition is always  
20 accompanied by high temperatures and an extremely fast heating rate. Therefore, the thermal pyrolysis technique  
21 is better suited for the study of the thermal decomposition of CR under these conditions; furthermore, pyrolysis  
22 products can be determined after the thermal pyrolysis technique is used in combination with GC/MS.  
23  
24  
25  
26  
27

28  
29 In the experiment, we first heat the pyrolyzer to the required temperature and then push the sample into the  
30 pyrolyzer by free fall to guarantee the pyrolysis of the sample under the set temperature. When the set pyrolysis  
31 time is reached, the pyrolysis products are brought by pyrolysis gas into the chromatographic spectrum to be  
32 separated and are then analyzed in the mass spectrometry system. The total ion chromatograms obtained after the  
33 thermal pyrolysis of CR at 200, 300, 400, 500 and 600 °C are shown in **Fig. 5**.  
34  
35  
36

37  
38 As shown in **Fig. 5**, only one base peak is present on the chromatogram at 200 °C when the retention time is  
39 20.97 min. Several small peaks are also present, and the retention time of each peak is essentially the same at 300,  
40 400 and 500 °C. At 600 °C, a new peak appears when the retention time is 1.67 min. After gas phase  
41 chromatography separation and mass spectrometry identification, the mass spectra of the pyrolysis products of  
42 each temperature are shown in **Fig. 6** for the same products, and the spectrum obtained after combining artificial  
43 analysis of a spectrum database is shown in **Table 4**. The results show that CR does not decompose at 200°C and  
44 that its decomposition products are identical at 300°C, 400°C and 500°C; at 600°C, CO<sub>2</sub> is the only new  
45 decomposition product.  
46  
47  
48  
49  
50  
51

52  
53 Based on **Figs. 5** and **6** and **Table 4**, it can be deduced that the first step in the thermal pyrolysis of CR  
54 occurs between 200 and 300 °C. The products of thermal pyrolysis between 300 and 500 °C are 2-aminodiphenyl  
55 ether and 10, 11-dihydrodibenz [b, f] [1, 4] oxazepin-11-one. At 600 °C, a new peak appears in the chromatogram  
56 due to the presence of CO<sub>2</sub>. The peak values and areas of products of the decomposition in the chromatograms at  
57  
58  
59  
60

various temperatures are smaller than those for CR without pyrolysis, which probably occurred because the volume of CR in the decomposition container was too high and some CR entered the chromatographic instrument without being decomposed. Air is used as the thermal pyrolysis atmosphere in this experiment. At the highest temperature used in this experiment, 600 °C, the benzene rings of CR cannot be split, and 10,11-dihydrodibenz(b,f) (1,4)oxazepin-11-one is the product of CR oxidation. 2-Aminodiphenyl ether is formed after the bond in CR is split. Further, CO<sub>2</sub> was observed. Its appearance was likely due to the oxidation of the organic decomposition products.

## Conclusions

In this study, upon heating under oxygen-free conditions at the rates of 2, 5 and 10 °C·min<sup>-1</sup>, CR fuses and absorbs heat at the temperature of approximately 69 °C without any mass loss. When the heating rate is 2 °C·min<sup>-1</sup>, the N=C-C bond in CR begins to pyrolyze and decomposes at the temperature of 172 °C; therefore, the heating rate has a relatively strong influence on the extrapolated initial decomposition temperature of CR, and the mechanism of the thermal decomposition is found to be described by the Zhuralev-Lesokin-Tempelmann equation,  $f(\alpha) = \frac{3}{2}(1-\alpha)^{\frac{4}{3}} \left[ (1-\alpha)^{\frac{1}{3}} - 1 \right]^{-1}$ . In the thermal pyrolysis experiment, the first step of CR thermal decomposition occurs between 200 and 300 °C. GC-MS can separate and analyze the products after pyrolysis and helps in studying the thermal decomposition mechanism of CR upon rapid heating. Through a combination of the experimental results obtained by thermoanalysis and thermal pyrolysis, it is found that for temperatures below 600 °C in the presence of oxygen, in addition to the pyrolysis reaction occurring to produce 2-Aminodiphenyl ether, the oxidizing reaction occurs to produce 10, 11-dihydrodibenz [b, f] [1, 4] oxazepin-11-one and carbon dioxide; however, the obtained products are independent of the temperature. It is suggested that the experimental results indicate that the burning temperature for the mixture of CR and the fireworks is not higher than 200 °C.

## References

- [1] R. Higginbottom and H. Suschitzky, *Chem. Soc.*, 1962, 2367-2370.
- [2] R. W. Foster and K. M. Weston, *Pain*, 1986, 25, 269-278.
- [3] E. J. Olajos and H. Salem, *Appl. Toxicol.*, 2001, 21, 355-391.
- [4] P. G. Blain, *Toxicol. Rev.*, 2003, 22, 103-110.
- [5] E. J. Olajos and W. Stopford, *Riot Control Agents: Issues in Toxicology, Safety & Health*, CRC Press, Boca Raton, 2004.
- [6] V. Pitschmann, *Toxins*, 2014, 6, 1761-1784.
- [7] G. H. Zhao, H. P. Chen and H. C. Dong, *Chemical Weapons*, Arms Industry Press, Beijing, 1991.
- [8] S. G. Hosseini, S. M. Pourmortazavi and S. S. Hajimirsadeghi, *Combust. Flame.*, 2005, 141, 322-326.
- [9] W. K. Lewis and C. G. Rumchik, *J. APPL. PHYS.*, 2009, 105, 056104.
- [10] L. L. Davis and K. R. Brower, *Phys. Chem.*, 1996, 100, 18775-18783.
- [11] Q. H. Lyu, L. S. Liu and Y. S. Liu, *Chin. Energ. Mater.*, 2012, 20, 218-222.

- 1  
2  
3 [12] X. Y. Wang and L.N. WANG, *Chin. Energ. Mater.*, 2013, 21, 103-107.  
4 [13] Y. R. Jorapur, G. Rajagopal, P.Saikia and R. R. Pal, *Tetrahedron. Lett.*, 2008, 49, 1495-1497.  
5 [14] H. Fakhraian, Y. Nafary, A. Yarahmadi, H. Hadj-Ghanbary and J. Heterocycl, *Chem*, 2008, 45, 1469-1472.  
6 [15] B. Ballantyne, *Toxicol*, 1977, 8, 347-379.  
7 [16] B. Brone, P. J. Peeters, R. Marrannes, M. Mercken, R. Nuydens, T. Meert, H.J.M. Gijssen and J. Toxicol, *Appl. Pharmacol.*,  
8 2008, 231, 150-156.  
9 [17] Z. Makles, M. Śliwakowski and M. Sokołowski, *Chemia. Analityczna.*, 1999, 44, 257-262.  
10 [18] M. Zuo and C. C. Liu, *Chin. Appl. Chem.*, 2008, 25, 1378-1380.  
11 [19] T. A. Kluchinsky, P. B. Savage, M. V. Sheely, R. J, *Microcol. Sep.*, 2001, 13, 186-190.  
12 [20] A. J. Kluchinsky, P. B. Savage, R. Fitz and P. A. Smith, *Am. Ind. Hyg. Assoc.*, 2002, 63: 493-496.  
13 [21] A. J. Kluchinsky, M. V. Sheely, P. B. Savage and P. A. Smith, *Chromatogr*, 2002, 952, 205-213.  
14 [22] J. J. Hout, G. L. Hook, P. T. LaPuma and D.W. White, *Occup. Environ. Hyg.*, 2010, 7, 352-357..  
15 [23] X.G. Jin, L.Y. Huang and Y. Shi, *Pyrolysis Gas Chromatography Method and Application*, Chemical Industry Press, Beijing,  
16 2009.  
17 [24] H. E. Kissinger, *Anal. Chem.*, 1957, 29, 1702-1706  
18 [25] T. Ozawa, *Bull. Chem. Soc. Japan.*, 1965, 38, 1881-1886.  
19 [26] T. Ozawa, *Therm. Anal.*, 1970, 2, 301-324.  
20 [27] R. Z. Hu, Z. Q. Yang and Y. J. Liang, *Thermochim. Acta.*, 1988, 123, 135-151.  
21 [28] R. Z. Hu, S.L. Gao and F. Q. Zhao, *Thermal Analysis Kinetics*, Science Press, Beijing, 2008.  
22 [29] V. Šatava, and J. Šesták, *Therm. Anal. Calorim.*, 1975, 8, 477-489.  
23 [30] A. W. Coats, *Nature*, 1964, 201, 68-69.  
24 [31] R. K. Agrawal, *Therm. Anal.*, 1987, 32, 149-156.  
25 [32] S. Vyazovkin, A. K. Burnham, J. M. Criado, L. A. Pérez-Maqueda, C. Popescu and N. Sbirrazzuoli, *Thermochim. Acta.*, 2011,  
26 520, 1-19.  
27 [33] J. J. Zhang, R. F. Wang, S. P. Wang and J. Bai, *Chin. Anal. Chem.*, 2004, 32, 1371-1374.  
28  
29  
30  
31  
32  
33  
34  
35  
36  
37  
38  
39  
40  
41  
42  
43  
44  
45  
46  
47  
48  
49  
50  
51  
52  
53  
54  
55  
56  
57  
58  
59  
60

**Table 1.** Melting peak values and the extrapolated initial temperatures for different heating rates

Heating rate (°C/min)	Peak /onset temperatures (°C)	
	Melting	Decomposition
2	69.37	172.13
5	69.22	178.94
10	69.16	183.91

**Table 2.** Peak temperatures and kinetics parameters of CR at different heating rates

DTG peak	$\beta/^\circ\text{C}\cdot\text{min}^{-1}$			$E_k/\text{kJ}\cdot\text{mol}^{-1}$	$\ln A_k$	$r_k$	$E_o/\text{kJ}\cdot\text{mol}^{-1}$	$r_o$
	2	5	10					
temperature ( $T_p$ ) /°C	203.51	211.49	217.07	221.79	20.67	0.9994	218.56	0.9995

**Table 3.** Comparison of kinetics parameters obtained using four integral methods

Method	$\beta(\text{K}\cdot\text{min}^{-1})$	$E(\text{kJ}\cdot\text{mol}^{-1})$	$\ln A$	$r$
Ordinary	2	211.5709	22.0483	0.9832
	5	190.4816	19.7858	0.9805
	10	189.0271	19.7373	0.9795
Šatava- Šesták	2	208.3597	21.7249	0.9842
	5	188.3788	19.5588	0.9818
	10	187.0763	19.5214	0.9809
Coats- Redfern	2	211.5709	22.0323	0.9832
	5	190.4816	19.7677	0.9805
	10	189.0271	19.7189	0.9795
Coats- Redfern	2	211.5709	22.0476	0.9832
	5	190.4816	19.7849	0.9805
	10	189.0271	19.7364	0.9795

**Table 4.** Pyrolysis products of CR at the temperature of 200°C, 300°C, 400°C, 500 and 600°C

Temperature/°C	No.	Pyrolysis products	Molecular Formula	Retention Time /min
200	b	Dibenz[b,f][1,4]oxazepine	C <sub>13</sub> H <sub>9</sub> NO	21.16
300	a	2-Aminodiphenyl ether	C <sub>12</sub> H <sub>11</sub> NO	18.71
400	b	Dibenz[b,f][1,4]oxazepine	C <sub>13</sub> H <sub>9</sub> NO	21.16
500	c	10,11-Dihydrodibenz[b, f][1, 4]oxazepin-11-one	C <sub>13</sub> H <sub>9</sub> NO <sub>2</sub>	24.67
		Carbon dioxide	CO <sub>2</sub>	1.67
	a	2-Aminodiphenyl ether	C <sub>12</sub> H <sub>11</sub> NO	18.71
600	b	Dibenz [b, f] [1, 4] oxazepine	C <sub>13</sub> H <sub>9</sub> NO	21.16
	c	10,11-Dihydrodibenz [b, f] [1, 4] oxazepin-11-one	C <sub>13</sub> H <sub>9</sub> NO <sub>2</sub>	24.67

Note: The sequence numbers of **Table 4**, **Fig. 5** and **Fig. 6** are correspondence.

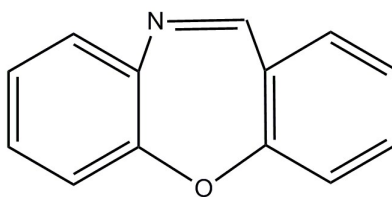


Fig. 1 The structure of CR

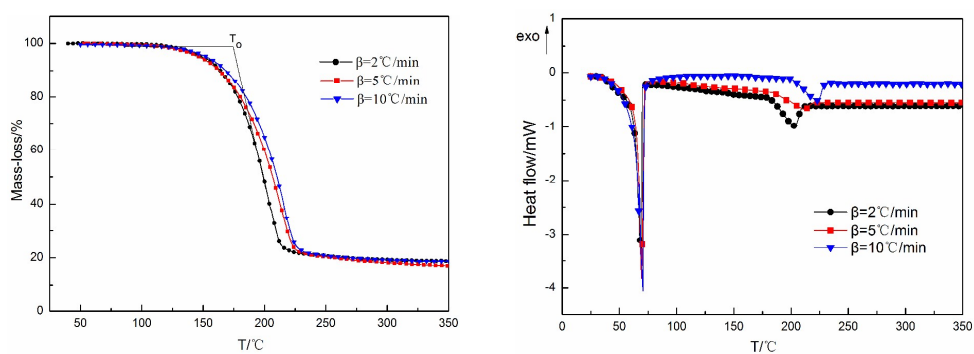


Fig. 2 TGA and DSC results for CR at different heating rates

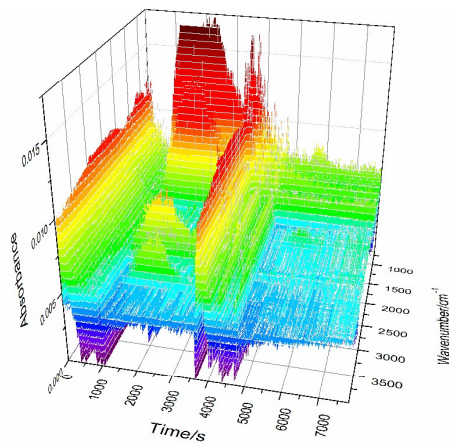


Fig. 3 3D FTIR spectra of gas products of CR during heating decomposition

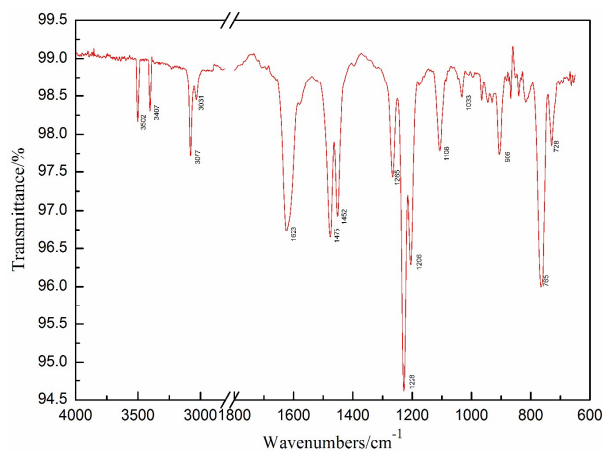
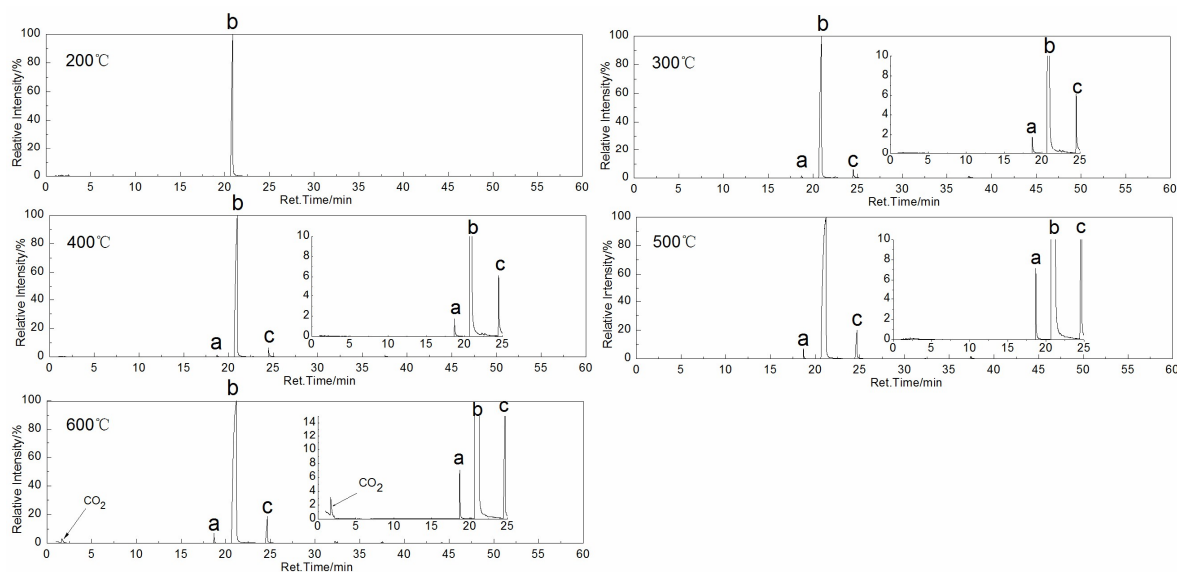
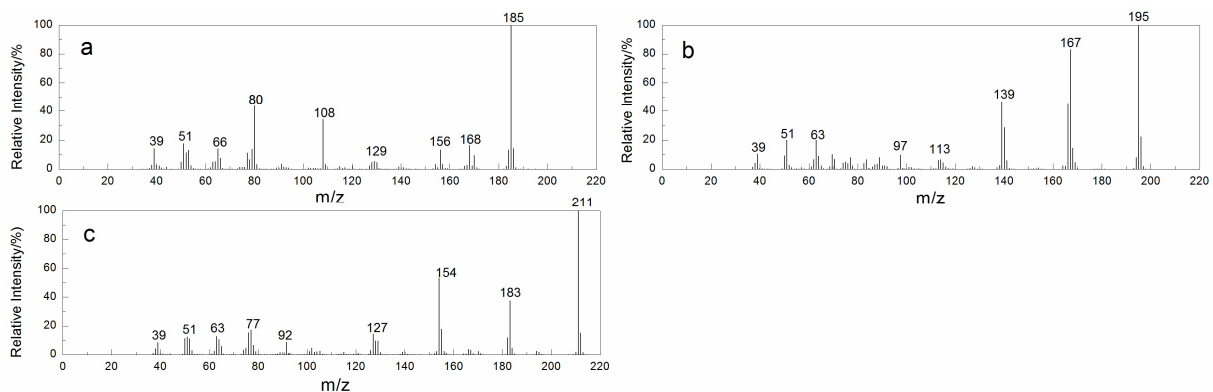


Fig. 4 2D FTIR spectrum at 2308s



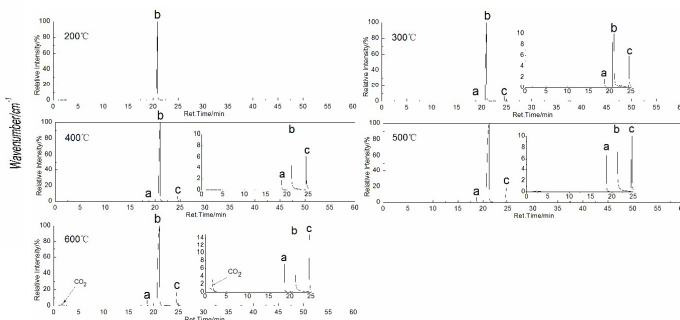
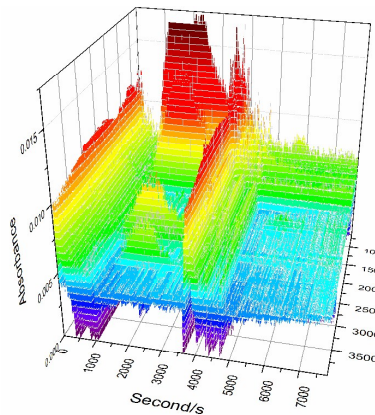
a: 2-Aminodiphenyl ether, b: Dibenz [b, f][1, 4] oxazepine, c: 10,11-Dihydrodibenz [b, f] [1, 4] oxazepin-11-one

Fig. 5 Ion flow of pyrolysis products of CR at 200, 300, 400, 500 and 600°C



a: 2-Aminodiphenyl ether, b: Dibenz [b, f] [1, 4] oxazepine, c: 10,11-Dihydrodibenz [b, f] [1, 4] oxazepin-11-one

Fig. 6 Mass spectra of the same pyrolysis products of CR at 300, 400, and 500°C



The mechanism function of the CR's thermal decomposition is Zhuravlev-Lesokin-Tempelmann equation. In air atmosphere, the pyrolysis reaction takes place to produce 2-aminodiphenyl ether, while the oxidizing reaction takes place to produce 10, 11-dihydrodibenz [b, f] [1, 4] oxazepin-11-one.